Journal of Environmental Management 323 (2022) 116200

Contents lists available at ScienceDirect

Journal of Environmental Management

journal homepage: www.elsevier.com/locate/jenvman

Research article

Assessing the protective effect of cutoff walls on groundwater pumping against saltwater upconing in coastal aquifers

Antoifi Abdoulhalik [a,**], Abdelrahman M. Abdelgawad [b], Ashraf A. Ahmed [c,*], Salissou Moutari [a], G. Hamill [d]

[a] School of Mathematics and Physics, Queen's University Belfast, University Road, Belfast, BT7 1NN, UK
[b] Civil Engineering Department, Faculty of Engineering, Assiut University, Asyut, Egypt
[c] Department of Civil & Environmental Engineering, Brunel University London, Kingston Lane, Uxbridge, UB83PH, UK
[d] School of Natural and Built Environment, Queen's University Belfast, University Road, Belfast, BT7 1NN, UK

ARTICLE INFO

Keywords:
Seawater intrusion
Subsurface barriers
Groundwater abstraction
Coastal aquifer management
Saltwater upconing
Pumping well salinisation
Laboratory experiments
Numerical modelling

ABSTRACT

Subsurface physical barriers are amongst the most effective methods to mitigate seawater intrusion in coastal aquifers. The main objective of this study was to examine the impact of cutoff walls on saltwater upconing using laboratory and numerical modelling experiments. Physical experiments were first completed to reproduce the saltwater upconing process in a laboratory-scale coastal aquifer model incorporating an impermeable cutoff wall. Numerical modelling was used for validation purposes and to perform additional simulations to explore the protective effect of cutoff walls against saltwater upconing. The results suggest that the cutoff wall did not substantially delay the saltwater upconing mechanism in the investigated configurations. Laboratory and numerical observations showed the existence of some residual saline water, which remained on the upper part of the aquifer on the seaward side of the wall following the retreat of the saltwater. The protective effect of cutoff walls was noticeably sensitive to the design parameters. Specifically, cutoff walls installed close to the pumping well enabled the implementation of higher pumping rates, therefore a more optimal use of the freshwater, especially for deeper wells. The results highlighted that the penetration depth of the cutoff walls may not necessarily need to exceed the depth of the pumping well to ensure effectiveness, which is of great importance from construction and economic perspectives.

1. Introduction

The landward encroachment of saline water in coastal aquifers, commonly known as seawater intrusion (SWI), has long been recognised as a worldwide environmental issue (Bear et al., 1999; Wu et al., 1993). Prompted by excessive groundwater abstraction coupled with climate-induced impacts, including drought and sea-level rise, SWI leads to negative impacts that are practically difficult to remediate. As saline water intrudes deeper into the aquifer system and approaches the location of the pumping wells, a large withdrawal of groundwater leads to the rise of the freshwater-saltwater interface below or within the vicinity of the well, a process known as the saltwater upconing mechanism (Reilly and Goodman, 1987; Abdelgawad et al., 2018; Abdoulhalik and Ahmed, 2018).

Amongst the quasi-irreversible effects caused by SWI, the most detrimental ones include the permanent abandonment of production wells and the salinisation of agricultural lands, coastal soils, as well as ecosystems (Werner et al., 2013; Badaruddin et al., 2015; Shi et al., 2020). SWI will continue to threaten and deteriorate coastal groundwater quality around the globe because the coastal population is expected to exceed 41% of the worldwide population, leading to increasing the groundwater abstraction (Martínez et al., 2007; Neumann et al., 2015; Yu et al., 2019), along with the forecasted rise of the sea level from 0.26 to 1.8 m by the end of the century (IPCC, 2013; Mahmoodzadeh and Karamouz, 2019). It is therefore of crucial importance to implement practical countermeasures to effectively protect groundwater pumping wells and enable more optimal and sustainable use of the remaining available coastal freshwater resources.

Amongst the most common methods used to mitigate saltwater intrusion is the implementation of subsurface barriers. These artificial

* Corresponding author.
** Corresponding author.
E-mail addresses: aabdoulhalik01@qub.ac.uk (A. Abdoulhalik), ashraf.ahmed@brunel.ac.uk (A.A. Ahmed).

https://doi.org/10.1016/j.jenvman.2022.116200
Received 25 May 2022; Received in revised form 4 September 2022; Accepted 4 September 2022
Available online 14 September 2022

barrier systems are installed along the coastline and can be of hydraulic or physical nature. Hydraulic barriers involve the injection of freshwater (positive barriers) and/or the abstraction of saltwater (negative barriers). Numerous studies have investigated their effectiveness as SWI control methods (Sherif and Hamza, 2001; Pool and Carrera, 2010; Luyun et al., 2011; Botero-acosta and Donado, 2015; Elsayed and Oumeraci, 2018). Physical barriers involve the construction of a low permeability wall to impede the landward encroachment of saline water. These may be installed on the upper part of the aquifer (i.e., cutoff walls) or in the lower part of the aquifer (i.e., subsurface dams).

Subsurface dams were found to have the potential to completely remove residual saline water from the inland storage area (Luyun et al., 2009; Abdoulhalik and Ahmed, 2017a; Chang et al., 2019). The effectiveness of cutoff walls in preventing SWI was well documented in several previous studies, both in homogeneous conditions (Luyun et al., 2011; Abdoulhalik et al., 2017; Anwar, 1983; Kaleris and Ziogas, 2013) and in more complex heterogeneous settings (Abdoulhalik and Ahmed, 2017b). Some studies had evidenced enhanced performance when a cutoff wall was combined with a semi-permeable dam (Abdoulhalik et., al 2017) or when associated with a hydraulic barrier (Armanuos et al., 2019).

While a number of laboratory and numerical studies have contributed to exploring the performance of cutoff walls against the encroachment of saline water into the aquifer (e.g., Luyun et al., 2011; Abdoulhalik and Ahmed, 2017b), little attention has been given to the assessment of their ability to protect freshwater abstraction wells from salinisation (e.g. Kaleris and Ziogas, 2013; Wu et al., 2020). Shen et al. (2020) have recently demonstrated the impact of cutoff walls on groundwater flow and salinity distribution in coastal aquifers under the influence of tidal activity. Sun et al. (2021) evidenced the substantial influence of cutoff walls on nitrate accumulation in upstream aquifers. Yang et al. (2021) have recently demonstrated the ability of cutoff walls to increase the size of freshwater lenses in coastal islands, which is of great relevance for the management of freshwater resources in islands where the risk of ocean-surge inundation is a serious potential threat.

Kaleris and Ziogas (2013) provided a thorough numerical analysis examining the impact of cutoff walls against SWI and groundwater withdrawals. Also, using numerical modelling tools, Wu et al., (2020) provided a comprehensive comparative analysis of the performance of underground barriers in preventing SWI and protecting groundwater abstraction by incorporating the third dimension, thereby extending previous analyses.

While the studies above have evidenced the effectiveness of cutoff walls, no previous studies have attempted to examine how cutoff walls would impact the saltwater upconing mechanism under controlled laboratory conditions. Therefore, the main purpose of this study was to examine the impact of cutoff walls on the saltwater upconing process using laboratory experiments combined with numerical simulations. The saltwater upconing process was first reproduced in a laboratory-scale coastal aquifer model incorporating an impermeable cutoff wall. The MODFLOW family SEAWAT model was then used for validation purposes and explore the sensitivity of the protective effect of cutoff walls to the main design parameters in order to determine the optimal cutoff wall configutation for a more optimal use of the freshwater resources.

2. Materials and method

2.1. Experimental method and procedure

A laboratory flow tank with the dimensions 0.38 m × 0.15 m x 0.01 m was used for the experiments. The tank consisted of a central chamber flanked by reservoirs on both sides, as shown in Fig. 1. The central chamber was filled with clear glass beads to simulate a homogeneous porous media. The mean diameter of the glass beads was 1090 μm, and the saltwater concentration was fixed at 28.96 g/L, which yields a density of 1020 kg/m3. The process of filling the tank with glass beads, preparing saltwater, estimating hydraulic conductivity, and calibration process were explained in more detail in Robinson et al. (2015) and Abdoulhalik et al. (2017).

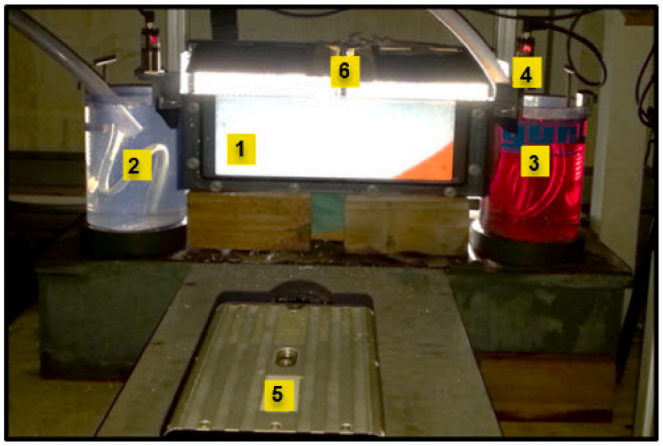

Fig. 1. Photograph of the experimental setup; 1) porous media chamber; 2) freshwater reservoir; 3) saltwater reservoir; 4) ultrasonic sensors; 5) high-speed camera; 6) LED lights.

The pumping well was simulated using a Terumo Neolus hypodermic needle connected by a flexible hose (Maprene) to a peristaltic pump Watson Marlow 101 U/R. The needle was 50 mm long with an outside and inside diameter of 1.1 mm and 0.7 mm, respectively. The internal diameter of the hose was 4.8 mm. The hose was maintained outside the porous media using a clamp supported by a retort stand placed behind the flow tank. The hose was carefully adjusted such that the tip of the needle was located 85 mm above the bottom of the tank and 190 mm away from the seaside boundary. The needle was kept in the same position in all the experiments. Plasticine was used to construct the cutoff wall, which was placed 108 mm deep and 60 mm away from the seaside boundary following the same procedure as in our previous investigations (e.g. Abdoulhalik and Ahmed, 2017a,b).

Three consecutive experiments were conducted with the same aquifer parameters and cutoff wall configurations: initial, upconing, and receding conditions. The initial condition experiment was simulated by applying a constant freshwater head of 135.7 mm. The overflow outlet in the saltwater reservoir was adjusted to maintain a constant head of 129.7 mm. No pumping took place during this experiment. This head difference of dh = 6 mm allowed the penetration of the dense saline water into the porous media until quasi-steady-state equilibrium. The second experiment (pumping condition) was initiated by turning on the pump at a fixed rate until the saltwater upconing mechanism was observed within a reasonable experimental time. The pump was then switched off to stop the abstraction and start the third experiment (receding condition), allowing the saltwater wedge to recede move back towards the seaside boundary.

2.2. Numerical model and procedure

The MODFLOW family variable flow code SEAWAT was used to perform the numerical simulations. The parameters adopted in these simulations are shown in Table 1. The dispersivity and element dimensions ensured numerical stability by meeting the Peclet number criterion (Voss and Souza, 1987; Abdoulhalik and Ahmed, 2017b). The left boundary was set as the constant head freshwater boundary of 135.7 mm, whereas a constant saltwater head of 129.7 mm was set at the right boundary. The time step was selected as 0.5 min, similar to that of the experiment. The simulation of the abstraction well was performed at the designated location when the initial steady-state was reached with a discharge rate of 0.49 ml/s for 50 mm until a quasi-steady-state

Table 1
Summary of the numerical parameters (lab-scale).

Input Parameters	Value
Aquifer parameters	
Domain length (cm)	38
Domain height (cm)	13
Element size (cm)	0.2
Hydraulic Conductivity (cm/min)	85
Porosity	0.3
Longitudinal dispersivity (cm)	0.1
Transversal dispersivity (cm)	0.01
Freshwater density (kg/m^3)	1000
Saltwater density (kg/m^3)	1020
Freshwater head (mm)	135.7
Saltwater head (mm)	129.7
Well configuration	
Well distance, L_w (cm)	19.0
Well depth, Z (cm)	8.5
Abstraction rates (mL/min)	29.4
Cutoff wall configuration	
Cutoff wall location L_c (cm)	6
Cutoff wall depth, H_c (cm)	10.8
Cutoff wall thickness (cm)	1
Cutoff wall hydraulic conductivity (cm/min)	0.0001

condition was obtained. The pumping was then stopped to initiate the retreat of the saltwater wedge in the last stress period. The parameters applied in the numerical simulations are summarised in Table 1.

3. Results and discussion

3.1. Experimental results

Fig. 2 shows the distribution of the salt concentration in the cutoff wall case and the base case, along with the transient toe length data. Before pumping, the horizontal extent of the saltwater wedge is visibly shorter in the barrier case, as expected.

The initiation of the pumping induced disruption of the equilibrium, causing the landward movement of the saltwater wedge. In the cutoff wall case, the obstruction of the seaward freshwater flow by the landward saline water filling the opening induced the free upward movement of the saline water on the seaward side of the wall, while the front of the wedge continued its landward progression and intersected the well (Fig. 2a). In the base case, the saltwater wedge gradually extended upward in the direction of the well until the freshwater-saltwater transition zone intersected the bore of the well (Fig. 2b). The saltwater upconing mechanism was observed in the two scenarios, albeit earlier in the cutoff wall case than in the base case. Specifically, the saltwater upconing process occurred within 55 min after pumping was initiated in the base case, while it was observed within 25 min in the cutoff wall case. This observation suggests that the cutoff wall installation induced an adverse effect in this specific configuration and caused earlier saltwater upconing compared to the base case; which is rather counterintuitive.

During the pumping, the initiation of the pumping induced disruption of the hydraulic equilibrium, causing the landward movement of the saltwater. The obstruction of the seaward freshwater flow by the landward saline water at the wall opening induced the free upward movement of the saline water along the seaside boundary while the front of the wedge gradually continued its progression toward the well.

The earlier occurrence of the saltwater upconing in the cutoff wall case is rather counterintuitive and suggests in that specific configuration and this given pumping rate the cutoff wall induced little effect against saltwater upconing. The sensitivity of the protective effect of cutoff walls to the main wall design parameters was thoroughly investigated using numerical modelling simulations, and the results are presented in section 4.

The widening of the upper portion of the freshwater-saltwater transition zone that is commonly observed during the saltwater upconing process was observed in both cases as the saltwater wedge approached the well (after 15 min), albeit the widening was more significant in the cutoff wall case. Besides, while the upconing process was rather continuous in the base case, the saltwater wedge in the cutoff wall case was nearly subdivided into two parts on either side of the wall. While the back part of the saltwater wedge rapidly moved upwards and nearly filled the entire thickness of the aquifer on the seaward side of the wall, the front part of the saltwater wedge slowly extended and moved upward toward the well until the upconing occurred.

The decay of the saltwater wedge was prompted upon switching off the pump, which caused an abrupt motion of the saline water towards the seaside boundary and regained its initial shape. Interestingly some residual saline water persisted for an extended period of time at the top right corner of the system before it was removed entirely at the final steady-state.

The transient toe length data presented in Fig. 2c shows that the migration rate of the tip of the wedge in the advancing phase was relatively similar in the two cases. After the pumping was stopped, the saltwater retreated towards the seaside boundary. The migration rate of the wedge tip during the receding phase was faster in the cutoff wall barrier case. In both cases, the toe length at the final steady-state was the same as the initial steady-state, which shows that no hysteresis occurred throughout the experiment. The data show that the receding rate of the toe was noticeably faster in the cutoff wall case than in the base case, as expected (Abdoulhalik et al., 2017). The higher flow velocity through the wall opening (e.g. Abdoulhalik and Ahmed, 2017a) caused the saltwater wedge length reduction in the cutoff wall case at the pre-pumping stage and induced significantly faster retreat following pumping shut-off.

3.2. Numerical modelling

3.2.1. Advancing phase

The numerical validation was based on both a qualitative comparison of the shape of the wedge at different times as well as a quantitative analysis of transient toe length data (Fig. 3). In the qualitative analysis, the shape of the wedge produced in the numerical model at various time points was compared to the observations made in the physical experiments (Fig. 3a and b). The quantitative analysis consisted in comparing the transient numerical toe length data to those recorded in the experiments of a time interval of 30 s (Fig. 3c). This double approach is more robust than the simple steady-state analysis performed in most previous studies. In addition, this comparative analysis was completed during both the advancing and the receding phases. The advancing phase referred to the landward movement of the wedge following the initiation of the pumping, and the saltwater upconing occurred. The receding phase referred to the decay of the saltwater wedge after the pumping was stopped.

The results show that the numerical model reproduced the shape of the saltwater wedge in all the various stages of the upconing mechanism observed in the experiments. The saltwater upconing process produced in the numerical model occurred almost at the same time as in the physical experiment. Some disparities could nonetheless be observed in the height of the saltwater wedge along the seaside boundary in the early stage of the advancing phase, nearby the position of the freshwater-saltwater transition zone ($t = 5$ min). This mismatch was probably due to the faster penetration of the saline water in the numerical model. The gradual widening of the transition zone at the front of the wedge during the upconing was relatively well depicted ($t = 10$ min and $t = 15$ min).

The final form of the upconing wedge was very well depicted, reproducing the evolution of the transition zone from wide to thin as the saltwater intersected the bore of the well. The comparison between the transient numerical and experiment toe length exhibited excellent agreement throughout the entire advancing phase (Fig. 3c). The

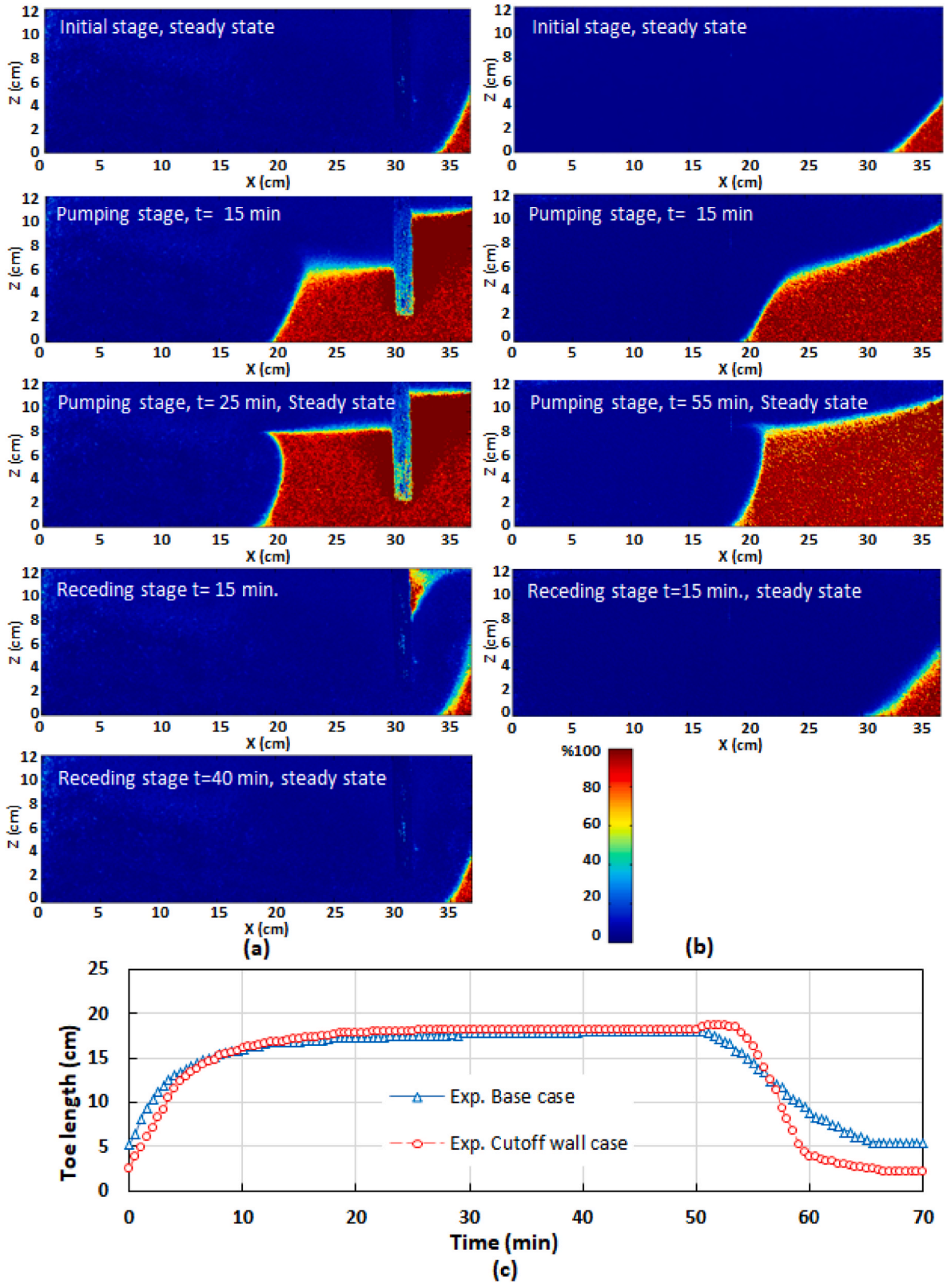

Fig. 2. Transient experimental results of the cutoff wall case (left) and the base case (right) for the initial, pumping, and receding stages: Concentration colour maps of the a) cutoff wall case and b) base case, c) Quantitative comparison between the cutoff wall case and base case (Q = 29.4 mL/min). (For interpretation of the references to colour in this figure legend, the reader is referred to the Web version of this article.)

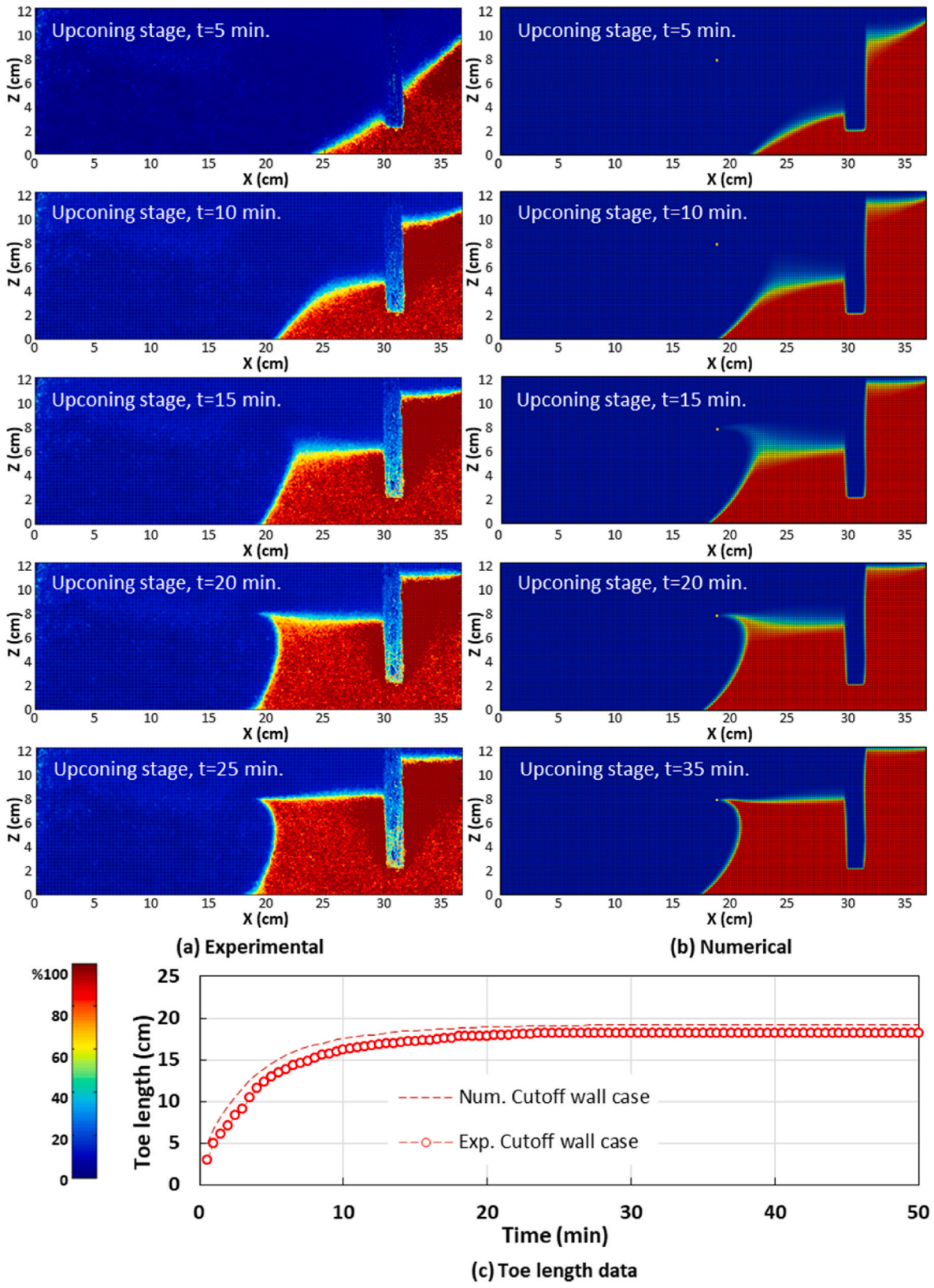

Fig. 3. Comparison between experimental (left) and numerical saltwater (right) upconing process (Q = 0.49 mL/s) (a) Experimental concentration colour maps (b) Numerical Images (c) Toe Length data. (For interpretation of the references to colour in this figure legend, the reader is referred to the Web version of this article.)

saltwater upconing process also occurred slightly earlier in the cutoff wall case than in the base case, which agrees with the experimental observations. While the freshwater-saltwater interface intersected the bore of the well within 30 min the base case (Fig. 4), some saline water already reached the well within less than 20 min in the cutoff wall case.

3.2.2. Receding phase

Fig. 5 shows the comparison between the experimental and numerical results of the receding phase. The numerical model images were compared to the detailed concentration colour maps produced from the physical experiments. They depicted the decay of the saltwater wedge very well after the pump was turned off (Fig. 5a and b). The model reproduced the widening of the transition zone, generally associated with seaward saltwater wedge movements (t = 3 min and t = 6 min). Fig. 5c shows that the transient experimental toe length results compared with the numerical prediction relatively well. The numerical model reproduced the slight landward shift of the toe prior to the retreat (t = 50 min).

As expected, the seaward motion of the toe was faster in the numerical model, as observed in similar previous studies. While the saltwater wedge toe required about 20 min to return to its initial location in the physical experiment, it took only 10 min in the numerical model. The numerical model also reproduced the phenomenon observed in the laboratory experiment, whereby some residual saline water persisted in the upper part of the aquifer upper part on the seaward side of the cutoff wall. This residual saline water was entirely flushed out within 50 min after the pumping was stopped, agreeing with the experimental observations.

3.3. Sensitivity analysis

Additional simulations were conducted to explore the sensitivity of the protective effect of cutoff walls to the main design parameters. The optimum cutoff wall configuration was considered to yield the maximum percentage increase in the critical pumping rate (the rate at which 1% salt contour line reaches the well) compared to the base case (without barrier). The main design parameters investigated herein included the depth of the cutoff wall H_C and its distance to the coastline X_C. For the sake of comprehensiveness, three different values of pumping well depth H_W were systematically tested. The aquifer dimensions and parameters were identical to those used in the physical and numerical models, as shown in Fig. 6.

The optimum cutoff wall configuration was herein considered to be the one producing the maximum percentage increase in the critical pumping rate (PC), defined by the following equation:

$$P_C = \frac{(Q_C - Q_{C\ base})}{Q_{C\ base}} \times 100,$$

where (Q_C) and (Q_C base) designate the critical pumping rates resulting from a given cutoff wall system and the base case, respectively; therefore, larger P_C values imply an improved well performance.

Dimensionless ratios characterised the main design parameters of the cutoff wall. The wall depth was expressed by the ratio (H_C/H), where H_C and H refer to the cutoff wall depth and the aquifer thickness, respectively. The location of the wall was expressed by the ratio (X_C/X_W), where X_C and X_W refer to the cutoff wall and well distances from the coastline, respectively. Furthermore, the pumping well depth was expressed by the ratio (H_W/H), where H_W is the depth of the pumping well screen.

Table 2 details the values of the cutoff wall and pumping well parameters adopted in the sensitivity analysis. Three well depths were tested, namely H_W/H = 0.35, 0.50, and 0.6, and for each of these scenarios, several cutoff wall configurations were examined. For each specific configuration, the critical pumping rate was adopted after trials and errors, whereby the pumping rate was gradually increased with an incremental step of 0.1 mL/min until the 1% salt contour line reached the well. In all the simulations, the initial condition corresponded to that of a steady-state saltwater wedge associated with a head difference dh = 6 mm. The abstraction was then initiated until the 1% salt contour line reached the well. The pumping was finally turned off to allow the retreat of the saline water.

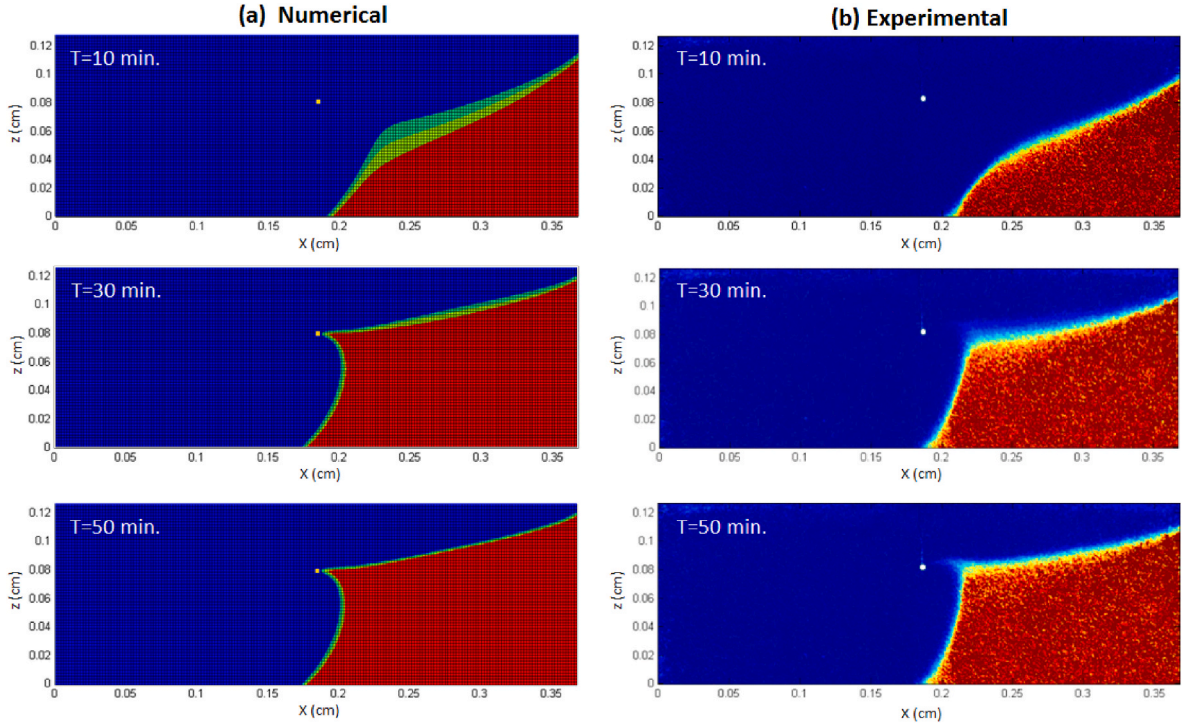

Fig. 4. Comparison between experimental and numerical saltwater upconing process (Q = 0.49 mL/s) in base case (without barrier) from Abdelgawad et al. (2018).

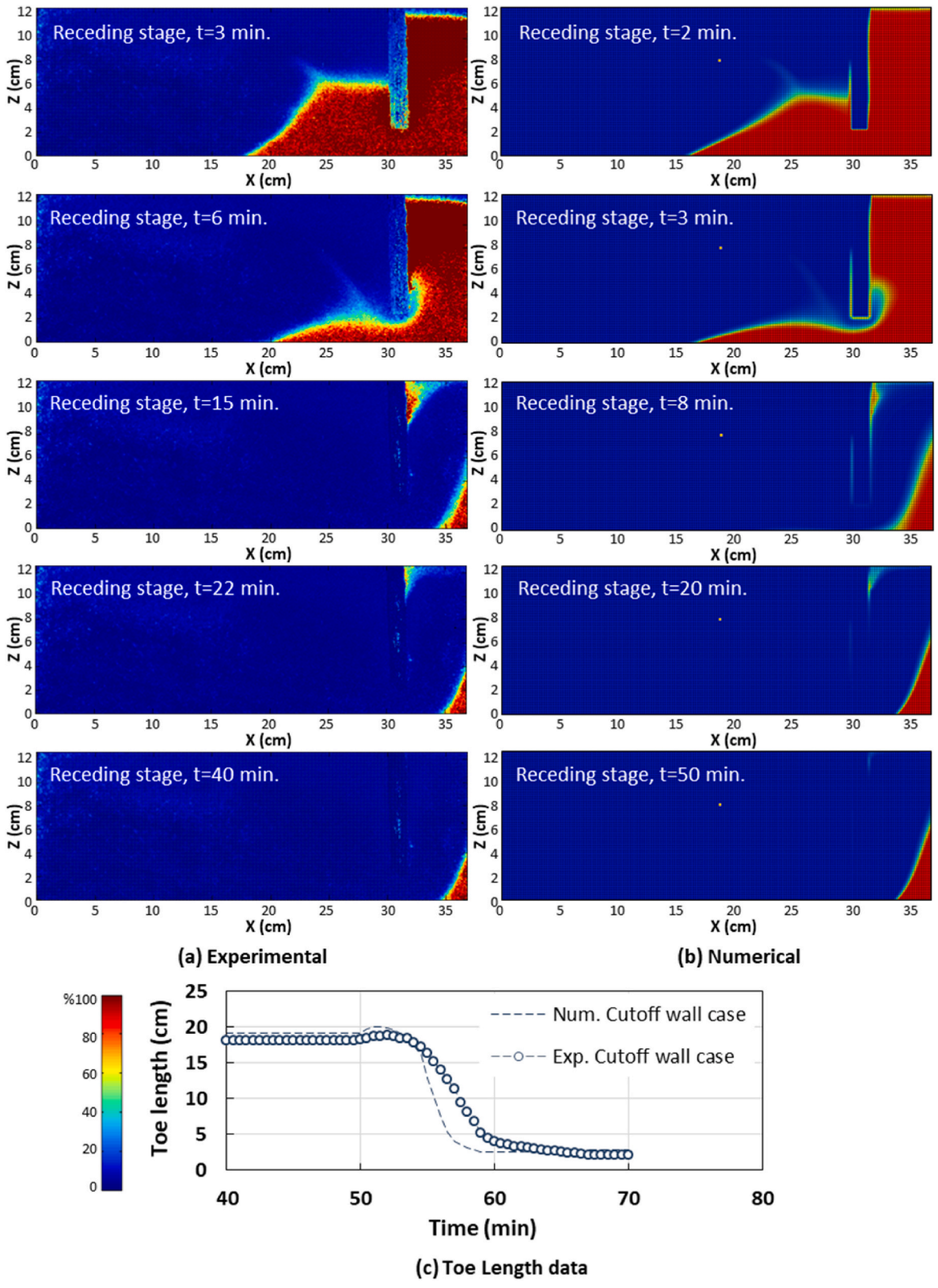

Fig. 5. Comparison between experimental and numerical saltwater receding process (a) Experimental concentration colour maps (b) Numerical Images (c) Toe Length data. (For interpretation of the references to colour in this figure legend, the reader is referred to the Web version of this article.)

3.3.1. Sensitivity to the cutoff wall location

In this section, a total of 12 values of X_C/X_W were tested. The penetration depth of the cutoff wall was fixed such that $H_C/H = 0.83$, i.e., the cutoff wall was placed at different locations over the horizontal length of the aquifer, while the tip of the wall remained at the same depth. For each scenario, three well depth values were tested for the sake of comprehensiveness, namely $H_W/H = 0.35$, 0.5, and 0.65. While smaller X_C/X_W values represent the cases where the cutoff wall is closer

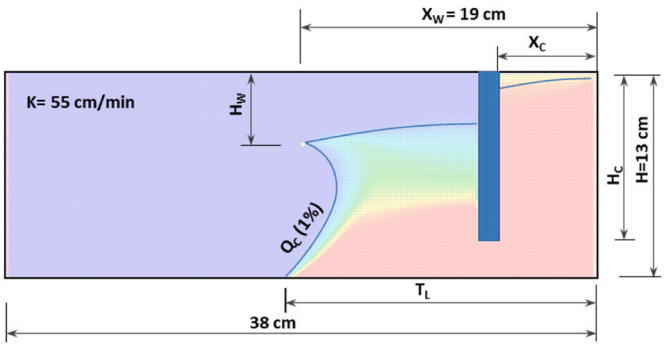

Fig. 6. Schematic diagram of the saltwater upconing wedge showing the various parameters considered in the sensitivity analysis.

Table 2
Variables of the cutoff wall and pumping well configurations.

Parameters	Values
Aquifer parameters	
Aquifer dim. (cm)	38 x 13
Hydraulic conductivity, K (cm/min)	55
Saline water density (kg/m3)	1020
α_T (cm)	0.05
α_L(cm)	0.1
Well configurations	
Well distance, X_W (cm)	19
Well depth ratio, H_W/H	0.35, 0.5, 0.65
Pumping rate Q (mL/min)	Increment every 0.05
Cutoff wall configurations	
Depth ratio, H_C/H	0.2, 0.31, 0.4, 0.51, 0.6, 0.71, 0.83 and 0.9
Location ratio, X_C/X_W	0.07, 0.14, 0.23, 0.33, 0.42, 0.52, 0.61, 0.71, 0.75, 0.80, 0.85, 0.89, and 1.00

to the seaside boundary, higher X_C/X_W values mean that the cutoff wall is placed closer to the pumping well. The results are presented in Fig. 7.

Fig. 7 shows the effect of the cutoff wall location on the critical pumping rate. The results show for equivalent cutoff wall distance, shallower pumping wells led to higher critical pumping rate values. In all pumping well depth scenarios, increasing the distance between the cutoff wall and the seaside boundary induced little noticeable decrement in the critical pumping rate but caused an abrupt increase as the cutoff wall approached the close vicinity of the well, albeit less visible for $H_W/H = 0.65$. This sharp change in trend was more significant for the shallow well scenario ($H_W/H = 0.35$). Fig. 7b shows that the stages of the upconing process differ significantly as the cutoff wall approaches the well location. Cutoff walls located farther away from the seaside boundary first induce saltwater buildup on the seaward side of the wall before it approaches the well, thereby delaying the upconing. The pumping rate required for saltwater upconing to occur was higher for the cutoff wall placed close to the pumping well.

To quantify the effectiveness of cutoff wall location on the critical pumping rate, all cutoff wall location cases were compared with the base cases for every well depth scenario and the results are presented in Table 3. The results show that higher P_C values were obtained for deeper wells, i.e., the cutoff walls added a substantial contribution to the optimal use of freshwater for deeper pumping wells. The data show that Pc values slightly decreased with increasing distance to the coastline until the cutoff wall is within the vicinity of the well, i.e., $X_C/X_W = 0.8$ for $H_W/H = 0.35$ and 0.5 $X_C/X_W = 0.85$ for $H_W/H = 0.65$. In other words, cutoff walls installed close to the well enabled the implementation of higher pumping rates, therefore more optimal use of the freshwater.

3.3.2. *Sensitivity to the cutoff wall depth*

To investigate the sensitivity of the critical pumping rate to the cutoff wall depth, a total of 8 values of the ratio H_C/H were analysed while the location of the cutoff wall was fixed such that $X_C/X_W = 0.33$. For each scenario, three well depth values were tested such that $H_W/H = 0.35$, 0.5 and 0.65. The results are presented in Fig. 8.

Fig. 8a shows that the critical pumping rate increased with increasing cutoff wall depth, especially for the deeper pumping well scenarios (i.e., $H_W/H = 0.5$ and 0.65). Hence, the pumping rate at which saltwater upconing occurred was higher for deeper cutoff walls for a given pumping well depth. This may be because deeper cutoff walls caused more disruption of the landward saline water movement and facilitated saltwater buildup on the seaward side of the wall, thereby delaying the occurrence of the saltwater upconing mechanism (Fig. 8b). The impact of the cutoff wall depth on the critical pumping rate was higher for deep wells than for shallower wells.

Table 4 shows the percentages of change in the critical pumping rate, Pc, in different well depth scenarios. The data show the continuous increase of this percentage with increasing cutoff wall depth. Hence, the

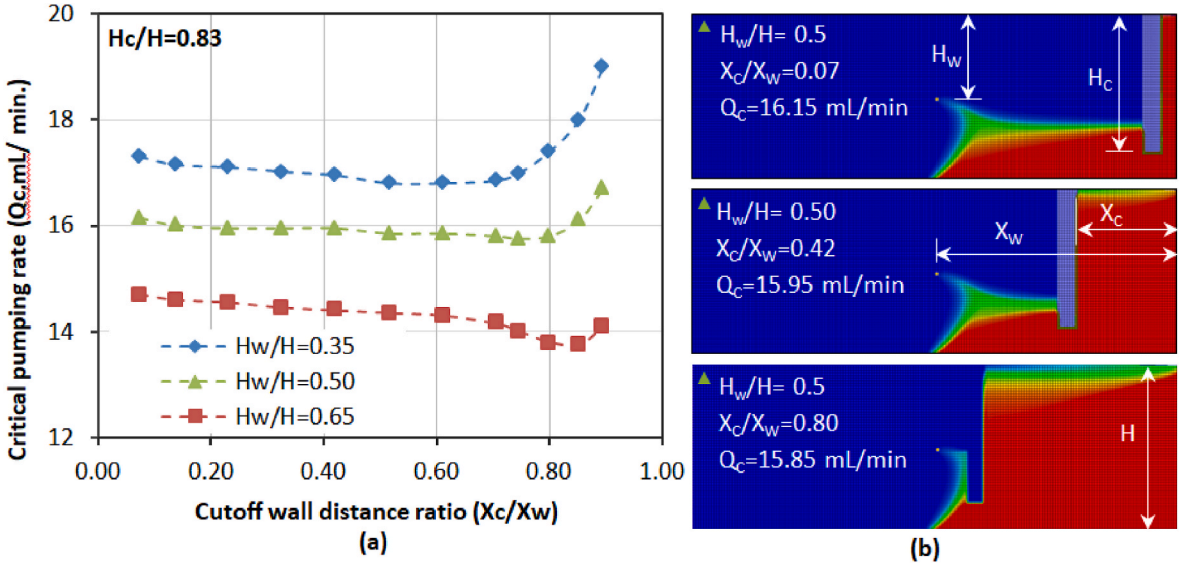

Fig. 7. (a) Sensitivity of the critical pumping rate to the cutoff wall distance, (b) Numerical steady-state images of three cutoff wall location at the second well depth scenario ($H_W/H = 0.5$).

Table 3
Percentage increase PC for the different cutoff wall locations tested.

$$P_C = \frac{(Q_C - Q_{C\,base})}{Q_{C\,base}} \times 100\ (\%)$$

	(X_c/X_W)	0.07	0.14	0.23	0.33	0.42	0.52	0.61	0.71	0.80	0.85	0.89
H_W/H	**0.35**	5.17	4.26	3.95	3.47	3.04	2.43	2.13	2.13	5.78	9.42	15.50
	0.50	16.19	15.11	14.75	14.75	14.75	14.03	14.03	13.67	13.67	15.83	20.14
	0.65	30.09	29.20	28.76	27.88	27.43	26.99	26.55	25.22	22.12	21.68	24.78

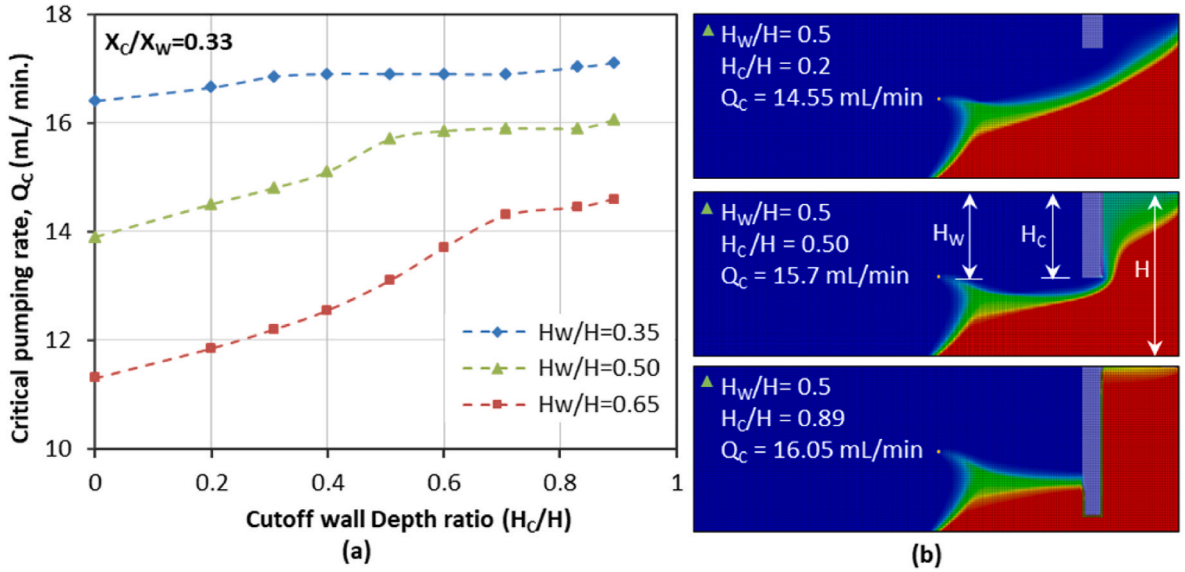

Fig. 8. (a) The relation between cutoff wall depth ratio and the critical pumping rate at three different well depth ratio, (b) Steady-state numerical images of some selected cutoff wall depth ratio cases at the second well depth scenario ($H_W/H = 0.5$).

Table 4
Percentage increase PC for the various wall penetration depth values tested.

$$P_C = \frac{(Q_C - Q_{C\,base})}{Q_{C\,base}} \times 100\ (\%)$$

	Hc/H	0.20	0.31	0.40	0.51	0.60	0.71	0.83	0.90
H_W/H	**0.35**	1.5	2.75	3.05	3.05	3.05	3.05	3.8	4.2
	0.5	4.3	6.5	8.6	13.0	14.03	14.4	14.4	15.5
	0.65	4.9	8	11.05	15.9	21.2	26.5	27.8	29.2

saltwater upconing mechanism occurred faster for shorter wall penetration depths for a fixed well configuration and equivalent pumping rate increment. In other words, deeper cutoff walls enable more optimal abstraction of freshwater. For the well depth scenarios of $H_W/H = 0.35$, 0.5, and 0.65, the highest PC values were 4.2%, 15.5%, and 29.2%, respectively. Those values show that the greater the well depth, the greater the cutoff wall impact on the critical pumping rate.

It is interesting to note that the increasing rate of the critical pumping rate Q_C (Fig. 8a) and the percentage increase P_C (Table 4) lowered as soon as the depth of the cutoff wall approached the depth of the corresponding well. In other words, the influence of the penetration depth on the protective effect of cutoff walls was limited for wall depths extending the depth of the pumping well. These results extend the findings reported by Kaleris and Ziogas (2013), who reported that the protective effect of the cutoff walls against pumping well salinisation increased with increasing wall penetration depth. These results, therefore, imply that to ensure effective protection of freshwater abstraction wells, it may be sufficient to build cutoff walls with the same penetration depth as the depth of the pumping wells, which is of great relevance from construction and economic standpoint.

4. Summary and conclusions

This investigation presented a quantitative analysis of the protective effect of cutoff walls on coastal groundwater abstraction against saltwater upconing mechanism using a laboratory-scale aquifer model. Numerical modelling was used for validation and to explore the sensitivity of the protective effect of cutoff walls to the main design parameters, whereby the optimum cutoff wall configuration was considered as the one yielding the maximum percentage of increase in the critical pumping rate (the rate at which 1% salt contour line reaches the well) compared to the base case (without barrier).

Both experimental and numerical results suggest that in the investigated configuration the cutoff wall induced did not substantially delayed saltwater upconing mechanism. Laboratory and numerical observations showed, for the first time, the existence of some residual saline water that remained on the upper part of the aquifer on the seaward side of the wall following the retreat of the saltwater, which was gradually flushed out of the system.

The protective effect of the cutoff wall was noticeably sensitive to the design parameters of the cutoff walls. The results show that the

percentage increase slightly decreased with increasing distance to the coastline until the cutoff wall reaches the vicinity of the well. In other words, cutoff walls installed close to the well enabled higher pumping rates, therefore more optimal use of the freshwater. Also, higher percentage increase were obtained for deeper wells, i.e., the cutoff walls added a substantial contribution to the optimal use of freshwater where pumping wells had greater depth.

The results also show that increasing wall penetration depth induced higher percentage increase. Hence, the protective effect of cutoff walls against well salinisation was better for deeper cutoff walls, which allowed more optimal freshwater abstraction. Interestingly, the numerical analysis evidenced that the influence of the penetration depth on the protective effect of cutoff walls was limited for wall depths extending beyond the pumping well depth. These findings imply that to ensure effective protection of freshwater abstraction wells, it may be enough to build cutoff walls with the same penetration depth as the corresponding pumping wells; this is of great importance and relevance from construction and economic perspective.

Credit author statement

Antoifi Abdoulhalik: Conceptualization, Methodology, Investigation, writing original draft. **Ashraf Ahmed**: Conceptualization, Supervision, review and editing, **Salissou Moutari**: Supervision, review and editing, **A Abdelgawad**: Numerical modelling, review and editing, **G Hamill**: Methodology, Supervision.

Declaration of competing interest

The authors declare that they have no known competing financial interests or personal relationships that could have appeared to influence the work reported in this paper.

Data availability

No data was used for the research described in the article.

References

Abdelgawad, A.M., Abdoulhalik, A., Ahmed, A., Moutari, S., Hamill, G.A., 2018. Transient investigation of the critical abstraction rates in coastal aquifers : numerical and experimental study. Water Resour. Manag. 32, 3563–3577. https://doi.org/10.1007/s11269-018-1988-3.

Abdoulhalik, A., Ahmed, A.A., 2017a. The effectiveness of cutoff walls to control saltwater intrusion in multi-layered coastal aquifers: experimental and numerical study. J. Environ. Manag. 199, 62–73. https://doi.org/10.1016/j.jenvman.2017.05.040.

Abdoulhalik, A., Ahmed, A.A., 2017b. How does layered heterogeneity affect the ability of subsurface dams to clean up coastal aquifers contaminated with seawater intrusion? J. Hydrol. 553, 708–721. https://doi.org/10.1016/j.jhydrol.2017.08.044.

Abdoulhalik, A., Ahmed, A.A., 2018. Transient investigation of saltwater upconing in laboratory-scale coastal aquifer. Estuar. Coast Shelf Sci. 214, 149–160. https://doi.org/10.1016/j.ecss.2018.09.024.

Abdoulhalik, A., Ahmed, A., Hamill, G.A., 2017. A new physical barrier system for seawater intrusion control. J. Hydrol. 549, 416–427. https://doi.org/10.1016/j.jhydrol.2017.04.005.

Anwar, H., 1983. The effect of a subsurface barrier on the conservation of freshwater in coastal aquifers. Water Res. 17, 1257–1265. https://doi.org/10.1016/0043-1354(83)90250-6.

Armanuos, A.M., Ibrahim, M.G., Mahmod, W.E., Takemura, J., Yoshimura, C., 2019. Analysing the combined effect of barrier wall and freshwater injection countermeasures on controlling saltwater intrusion in unconfined coastal aquifer systems. Water Resour. Manag. 33, 1265–1280. https://doi.org/10.1007/s11269-019-2184-9.

Badaruddin, S., Werner, A.D., Morgan, L.K., 2015. Watertable salinisation due to seawater intrusion. Water Resour. Res. 51 (10), 8397–8408. https://doi.org/10.1002/2015WR017098.

Bear, J., Cheng, A.H.D., Sorek, S., Ouazar, D., Herrera, I., 1999. Seawater Intrusion in Coastal Aquifers: Concepts, Methods and Practices. Kluwer, Dordrecht, The Netherlands.

Botero-acosta, A., Donado, L.D., 2015. Laboratory scale simulation of hydraulic barriers to seawater intrusion in confined coastal aquifers considering the effects of stratification. Procedia Environ. Sci. 25, 36–43. https://doi.org/10.1016/j.proenv.2015.04.006.

Chang, Q., Zheng, T., Zhenga, X., Zhang, B., Sun, Q., Walther, M., 2019. Effect of subsurface dams on saltwater intrusion and fresh groundwater discharge. J. Hydrol. 576, 508–519. https://doi.org/10.1016/j.jhydrol.2019.06.060.

Elsayed, S.M., Oumeraci, H., 2018. Modelling and mitigation of storm-induced saltwater intrusion : improvement of the resilience of coastal aquifers against marine floods by subsurface drainage. Environ. Model. Software 100, 252–277. https://doi.org/10.1016/j.envsoft.2017.11.030.

International Panel on Climate Change (IPCC), 2013. The Physical Science Basis. Working Group 1 Contribution to the Fifth Assessment Report of the International Panel on Climate Change (Cambridge, New York).

Kaleris, V.K., Ziogas, A.I., 2013. The effect of cutoff walls on saltwater intrusion and groundwater extraction in coastal aquifers. J. Hydrol. 476, 370–383. https://doi.org/10.1016/j.jhydrol.2012.11.007.

Luyun, R., Momii, K., Nakagawa, K., 2009. Laboratory-scale saltwater behavior due to subsurface cutoff wall. J. Hydrol. 377, 227–236. https://doi.org/10.1016/j.jhydrol.2009.08.019.

Luyun, R., Momii, K., Nakagawa, K., 2011. Effects of recharge wells and flow barriers on seawater intrusion. Ground Water 49, 239–249. https://doi.org/10.1111/j.1745-6584.2010.00719.x.

Mahmoodzadeh, D., Karamouz, M., 2019. Seawater intrusion in heterogeneous coastal aquifers under flooding events. J. Hydrol. 568, 1118–1130. https://doi.org/10.1016/j.jhydrol.2018.11.012.

Martínez, M.L., Intralawan, A., Vázquez, G., Pérez-Maqueo, O., Sutton, P., Landgrave, R., 2007. The coasts of our world: ecological, economic and social importance. Ecol. Econ. 63, 254–272. https://doi.org/10.1016/j.ecolecon.2006.10.022.

Neumann, B., Vafeidis, A.T., Zimmermann, J., Nicholls, R.J., 2015. Future coastal population growth and exposure to sea-level rise and coastal flooding – a global assessment. PLoS One 10, 34. https://doi.org/10.1371/journal.pone.0118571.

Pool, M., Carrera, J., 2010. Dynamics of negative hydraulic barriers to prevent seawater intrusion. Hydrogeol. J. 18, 95–105. https://doi.org/10.1007/s10040-009-0516-1.

Reilly, T.E., Goodman, A.S., 1987. Analysis of saltwater upconing beneath a pumping well. J. Hydrol. 89, 169–204. https://doi.org/10.1016/0022-1694(87)90179-X.

Robinson, Gareth, Hamill, G, Ahmed, Ashraf, 2015. Automated image analysis for experimental investigations of salt water intrusion in coastal aquifers. J. Hydrol. 530, 350–360. https://doi.org/10.1016/j.jhydrol.2015.09.046.

Shen, Y., Xin, P., Yu, X., 2020. Combined effect of cutoff wall and tides on groundwater flow and salinity distribution in coastal unconfined aquifers. J. Hydrol. 581, 124444 https://doi.org/10.1016/j.jhydrol.2019.124444.

Sherif, M., Hamza, K., 2001. Mitigation of seawater intrusion by pumping brackish water. Transp 34, 29–44. https://doi.org/10.1023/A:1010601208708. Porous Media.

Shi, W., Lu, C., Werner, A.D., 2020. Assessment of the impact of sea-level rise on seawater intrusion in sloping confined coastal aquifers. J. Hydrol. 586, 124872 https://doi.org/10.1016/j.jhydrol.2020.124872.

Sun, Q., Zheng, T., Zheng, X., Walther, M., 2021. Effectiveness and comparison of physical barriers on seawater intrusion and nitrate accumulation in upstream aquifers. J. Contam. Hydrol. 243, 103913 https://doi.org/10.1016/j.jconhyd.2021.103913.

Voss, C.I., Souza, W.R., 1987. Variable density flow and solute transport simulation of regional aquifers containing a narrow freshwater-saltwater transition zone. Water Resour. Res. 23, 1851–1866. https://doi.org/10.1029/WR023i010p01851.

Werner, A.D., Bakker, M., Post, V.E.A., Vandenbohede, A., Lu, C., Ataie-Ashtiani, B., Simmons, C.T., Barry, D.A., 2013. Seawater intrusion processes, investigation and management: recent advances and future challenges. Adv. Water Resour. 51, 3–26. https://doi.org/10.1016/j.advwatres.2012.03.004.

Wu, H, Lu, C, Kong, J, Werner, A, 2020. Preventing seawater intrusion and enhancing safe extraction using finite-length, impermeable subsurface barriers: 3D analysis. Water Resour. Res. 56 https://doi.org/10.1029/2020WR027792.

Wu, J., Xue, Y., Liu, P., Wang, J., Jiang, Q., Shi, H., 1993. Seawater intrusion in the coastal Area of Laizhou Bay, China: 2. Seawater intrusion monitoring. Ground Water 31, 740–745. https://doi.org/10.1111/j.1745-6584.1993.tb00845.x.

Yang, J., Graf, T., Luo, J., Lu, C., 2021. Effect of cutoff wall on freshwater storage in small islands considering ocean surge inundation. J. Hydrol 603, 127143. https://doi.org/10.1016/j.jhydrol.2021.127143.

Yu, X., Xin, P., Lu, C., 2019. Seawater intrusion and retreat in tidally-affected unconfined aquifers: laboratory experiments and numerical simulations. Adv. Water Resour. 132, 103393 https://doi.org/10.1016/j.advwatres.2019.103393.